Logic Gates and Antisense DNA Devices Operating on a Translator Nucleic Acid Scaffold

Bella Shlyahovsky, Yang Li, Oleg Lioubashevski, Johann Elbaz, and Itamar Willner*

Institute of Chemistry, The Hebrew University of Jerusalem, Jerusalem 91904, Israel

ABSTRACT A series of logic gates, "AND", "OR", and "XOR", are designed using a DNA scaffold that includes four "footholds" on which the logic operations are activated. Two of the footholds represent input-recognition strands, and these are blocked by complementary nucleic acids, whereas the other two footholds are blocked by nucleic acids that include the horseradish peroxidase (HRP)-mimicking DNAzyme sequence. The logic gates are activated by either nucleic acid inputs that hybridize to the respective "footholds", or by low-molecular-weight inputs (adenosine monophosphate or cocaine) that yield the respective aptamer—substrate complexes. This results in the respective translocation of the blocking nucleic acids to the footholds carrying the HRP-mimicking DNAzyme sequence, and the concomitant release of the respective DNAzyme. The released product-strands then self-assemble into the hemin/G-quadruplex-HRP-mimicking DNAzyme that biocatalyzes the formation of a colored product and provides an output signal for the different logic gates.The principle of the logic operation is, then, implemented as a possible paradigm for future nanomedicine. The nucleic acid inputs that bind to the blocked footholds result in the translocation of the blocking nucleic acids to the respective footholds carrying the antithrombin aptamer. The released aptamer inhibits, then, the hydrolytic activity of thrombin. The system demonstrates the regulation of a biocatalytic reaction by a translator system activated on a DNA scaffold.

KEYWORDS: aptamer · DNAzyme · DNA · logic gate · thrombin · nanomedicine

Biological transformations in cells are regulated by information transfer processes that are triggered by external or internal stimuli.[1,2] Recent research efforts are directed toward the organization of molecular systems that perform information processing or programmed mechanical functions as a result of the application of external signals.[3−7] Different molecular-,[8−11] enzymatic-[12−15] and peptide-based[16] assemblies that perform logic operations were designed. The use of nucleic acids as functional biomaterials for information processing and programmed mechanical activities is, however, most attractive as a means to mimic biocatalytic transformations and biochemical pathways. The information encoded in the base sequence of nucleic acids provides instructions for base-pairing, reactivity toward enzymes (endonucleases or nicking enzymes), specific binding properties (aptamers),[17−20] and self-assembly into catalytic nucleic acids (DNAzymes and ribozymes).[21−23] These features were implemented to develop different nucleic acid-based logic circuits. For example, various logic gates were constructed by using single-stranded fluorogenic nucleic acids acting as cleavable substrates for short nucleic acids functioning as ribozymes.[24,25] Similarly, chained DNA-based logic gates were designed, and the activation of logic-gate cascades by immobilizing individual logic gates on a solid support was demonstrated.[26] Furthermore, the specific base-pairing of nucleic acids, the ligation of single-stranded DNA, and the sequence-specific reactivity of duplex DNA in the presence of appropriate enzymes led to the development of programmable and autonomous computing devices (automaton).[27,28] In these systems, information transfer from one state to another proceeds autonomously with "decision-making" capabilities. In addition to the implementation of the recognition and reactivity of nucleic acids for molecular computing and information processing, substantial recent research efforts are directed toward the development of "DNA machines".[29−32] These systems constitute tailored DNA structures that perform programmed mechanical operations, as a response to external stimuli. For example, DNA machines such as walkers,[33] tweezers,[34] gears,[35] and more[36] were designed. In fact, besides the fundamental interest in developing artificial biomolecular computational networks and devices that mimic complex biological processes, these systems hold promising practical implications. Such functional DNA structures were suggested as active components in future nanomedicine for the analysis of disease-related biomarkers, and *in situ* release of

*Address correspondence to willnea@vms.huji.ac.il.

Received for review January 29, 2009 and accepted May 27, 2009.

Published online June 9, 2009.
10.1021/nn900085x CCC: $40.75

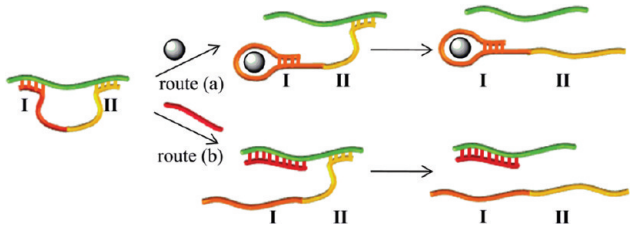

Scheme 1. The separation of a synergetically stabilized duplex DNA by the formation of an aptamer−substrate complex (route a) and by a nucleic acid strand displacement (route b).

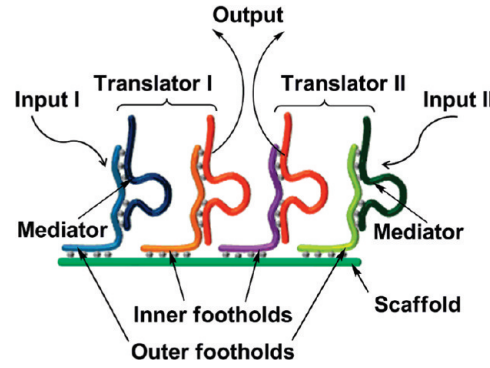

Scheme 2. Components of a logic gate construct on a DNA scaffold.

therapeutic counteragents.[37] Also, programmed DNA machines were used as active sensor devices.[38−40] It is, however, of great interest to combine the computational and mechanical functions of DNA-based devices to design modular and interconnected circuits.

Here we wish to report on the construction of DNA-based devices that perform AND, OR, and XOR logic gate operations. Besides the computational functions of the systems, we emphasize the future perspectives of such DNA devices for biomedicine, and specifically, we address the use of these machines for controlling the activity of an enzyme (the blood clotting thrombin).

RESULTS AND DISCUSSION

The inputs 1s and 0s of Boolean logics are represented by the presence or absence of a single stranded DNA molecule or aptamer substrates, respectively. For each gate, a different set of input strands or aptamer substrates satisfies the "true value" that results in the release of a catalytic nucleic acid that yields a readout signal.

Logic gates are constructed through a modular design that combines two DNA-translators in the device that performs logic operations. The DNA translators mediate the release of "product" nucleic acid strands in response to an "arbitrary" DNA-input strand, which does not exhibit complementarity to the product strand. This design allows us to decouple the input sequence from the sequence needed for the subsequent operations, and to utilize the translation of information encoded in the base sequences of DNA from one code to another.

The DNA translators described in the present study rely on three well-established features of nucleic acids:

(i) Nucleic acids with specific recognition properties toward low-molecular-weight substrates or proteins (aptamers) can be elicited.[17−20] The self-assembly of the aptamer−substrate complex may separate a duplex DNA structure, provided that the aptamer complex is energetically favored.

(ii) The stabilities of duplex nucleic acids are dominated by the extent of base-pairing. Specifically, duplex formation is facilitated by synergetic base-pairing of loop-bridged complementary domains I and II, Scheme 1. The separation of one of the duplex domains by the formation of an aptamer−substrate complex, Scheme 1, route a, or by the DNA strand displacement, Scheme 1, route b, as a result of favored affinity interactions, results in a weakened double-stranded domain II and the separation of the residual duplex structures that include the domain II. In contrast to the abundant strand displacement that proceeds from the single-stranded toe-hold,[41] located at the termini of a duplex template, in the present study strand displacement is initiated by duplex formation in the loop region.

(iii) Catalytic nucleic acids can be prepared (DNAzymes).[21−23] Specifically, we make use of a horseradish peroxidase (HRP)-mimicking DNAzyme[42,43] as a reporter for the activities of the DNA translator systems. That is, the release of the DNAzyme results in the biocatalyzed oxidation of 2,2′-azino-bis(3-ethylbenzothiazoline-6-sulfonic acid)-disodium salt, $ABTS^{2-}$, to the colored product $ABTS^{\cdot-}$.

The general construct for the activation of the logic gates constitutes four footholds that are hybridized to a common DNA scaffold acting as a "track", Scheme 2. Two "outer" footholds and two "inner" footholds, blocked by complementary nucleic acids, are assembled on the scaffold and yield two pairs of translators. The "outer" footholds are hybridized with "mediator-strands" and act as input-sensing units. Upon the activation of the systems by the respective inputs, the mediator-strands are translocated to the "inner" footholds, and the displacement of the nucleic acids linked to these footholds by the mediator-strands yield the released "product-strands". The catalytic DNAzyme features of the combined product-strands allow, then, the readout of the logic operations. It should be noted that all of the logic gate constructs are single-use devices.

In the first set of experiments, we implemented nucleic acids as inputs that activate a set of logic gate operations ("OR", "AND", and "XOR"). Figure 1A depicts the design of the "OR" logic gate using the DNA translator device. The principles to design the "OR" gate will be described in detail, and they will be adapted to construct all other systems described in the study. The sequence **1** is used as "track" on which the machine is as-

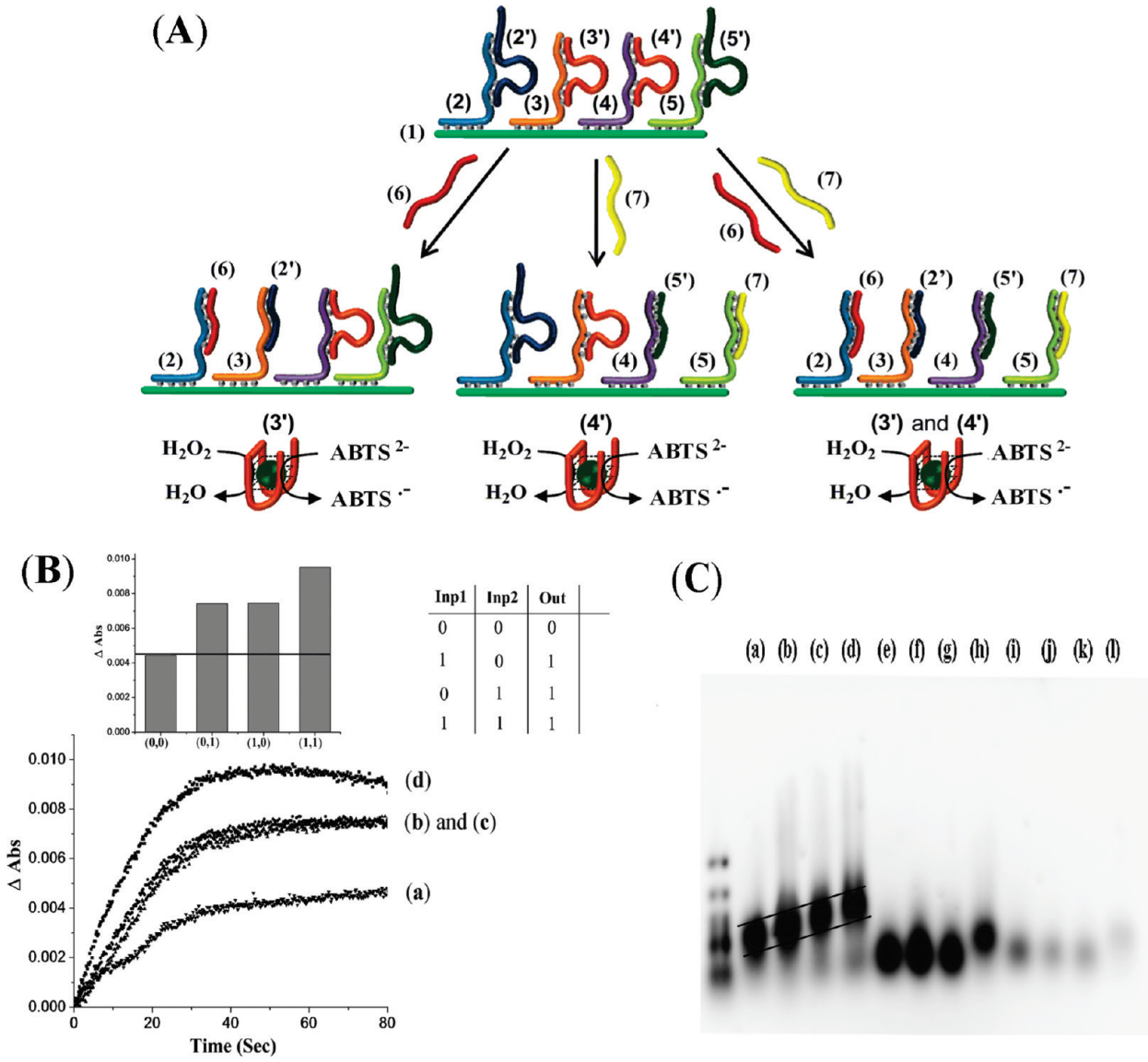

Figure 1. (A) Schematic presentation of an "OR" gate using a four-foothold nucleic acid structure on a DNA scaffold, and the activation of the logic gate by two-nucleic acids inputs. (B) Time-dependent absorbance changes stimulated by the released HRP-mimicking DNAzyme upon activation of the system by the respective nucleic acid inputs: (a) (0,0), (b) (0,1), (c) (1,0), (d) (1,1) (expressed as ΔAbs values, where ΔAbs corresponds to the difference between the absorbance generated by the input-activated system and the absorbance generated by hemin). Spectra recorded in the presence of hemin, 7×10^{-7} M, $ABTS^{2-}$, 2 mM, and H_2O_2 2 mM. Results are presented in the inset in the form of a bar presentation and the respective truth-table. (Note that the sequences 3′ and 4′ are identical, and separate numbering was used for clarity). (C) Agarose-gel electrophoretic image corresponding to the different structures consisting of scaffolds that include (a) one foothold, 2/2′, (b) two footholds, 2/2′ and 3/3′, (c) three footholds, 2/2′, 3/3′ and 4/4′, and (d) four footholds, 2/2′, 3/3′, 4/4′ and 5/5′. Entries e, f, g, and h depict the migration of the separate footholds 2/2′, 3/3′, 4/4′ and 5/5′, respectively, (in the absence of the scaffold 1). Entries i, j, k, and l depict the migration of the separate footholds 2/2′, 3/3′, 4/4′ and 5/5′ at the three times smaller concentrations compared to e, f, g, and h, respectively (in the absence of the scaffold 1).

sembled and operates. The four nucleic acids **2**, **3**, **4**, and **5** are hybridized with the "track", and these act as "footholds". The mediator-strands **2**′, **5**′ and product-strands **3**′, **4**′ are designed as loops that include binding arms that are only partially complementary to footholds **2**,**5** and **3**,**4**, respectively. The resulting structures are stabilized by synergetic hybridizations of the respective duplex domains. The mediator-strands **2**′ and **5**′ are also complementary, in part, to footholds **3** and **4**, but the enhanced base-pairing between **2**/**2**′ and **5**/**5**′ preserves them on footholds **2** and **5**, respectively.

In the "OR" gate, the product strands **3**′ and **4**′ include the sequence that can self-assemble in the presence of hemin into the G-quadruplex/hemin HRP-mimicking DNAzyme. The input nucleic acids **6** and **7** are partially complementary to footholds **2** and **5**, and since the base-pair complementarity of **6**/**2** and of **7**/**5** is higher than that of **2**′/**2** or **5**′/**5**, the treatment of the system with either **6** or **7**, results in the formation of the more stable **6**/**2** and **7**/**5** duplexes with the concomitant displacement of the mediator-strands **2**′ or **5**′, respectively. The displaced mediators **2**′ or **5**′ include,

however, superior base-pairing to footholds **3** and **4**, as compared to **3′** and **4′**, respectively, and thus, their release by the inputs stimulates their translocation to footholds **3** or **4**. The concomitant displacement of product strands **3′** and **4′** result in the self-assembly of the HRP-mimicking DNAzymes that, in the presence of hemin, catalyze the H_2O_2-mediated oxidation of $ABTS^{2-}$ to the colored product, $ABTS^{\bullet-}$. The absorption of colored product provides, then, the readout signal for the gate operation. As any of the DNA inputs **6** or **7**, as well as the two inputs together, activate the release of the HRP-mimicking DNAzymes, the system performs the "OR" logic gate operation.

Figure 1B depicts the time-dependent absorbance changes observed upon the activation of the "OR" gate with the inputs **6** or **7**, curves b and c, respectively, whereas curve d shows the absorbance changes in the presence of both inputs. The absorbance changes in the absence of the inputs, curve a, are due to residual DNAzyme units present in the solution. The absorbance changes in the form of bars and the truth table of the system are given in Figure 1B, inset.

A major aspect that needs to be addressed relates to the existence of the composite DNA scaffold on which the logic gates are activated. To address this point, we examined the different structures consisting of scaffolds that include one, two, three, and four footholds, hybridized with the respective mediator/DNAzyme strands on the DNA scaffolds by means of gel electrophoresis, Figure 1C. Entries a, b, c, and d correspond to the scaffold that includes one duplex foothold **2**/**2′**, the additional duplex foothold **3**/**3′**, the further added duplex foothold **4**/**4′**, and the system with the fourth duplex foothold **5**/**5′**, respectively, where all entries include the respective nucleic acid components at concentrations similar to those that used to study the "OR" logic gate. One may realize that the systems are well-resolved, and the four-footholds-scaffold structure reveals the lowest mobility. Entries e, f, g, and h depict the migration of the separate footholds **2**/**2′**, **3**/**3′**, **4**/**4′** and **5**/**5′**, respectively (in the absence of the scaffold **1**. All duplex footholds are examined at the same concentrations used in the entire "OR" gate construct. The duplex foothold **5**/**5′** migrates slightly slower than the other footholds, consistent with its higher weight. One may realize that in entries a−d the free duplex footholds are almost invisible, implying that the four-foothold/scaffold construct is the major component in the system. A detailed electrophoretic concentration-dependence study of the images of the footholds suggests that the concentration of the free footholds in the "OR" construct is in the range of 20−30%. It should be further noted that the precise ordering of the footholds on the scaffold is essential to reach the high-purity four-foothold construct (see also experimental section). This included the primary hybridization of the foothold **2**/**2′** on the scaffold. Subsequently, the preprepared footholds **3**/**3′**, **4**/**4′**, and **5**/**5′** were hybridized onto the **2**/**2′**-functionalized scaffold. Note that **2′** is also complementary to **3**, and **5′** is complementary to **4**. The resulting duplexes **2′**/**3** and **5′**/**4** are, however, energetically less stable than the duplexes **2**/**2′** and **5**/**5′**, and thus, the procedure to construct the gate composite eliminates undesirable crossovers, consistent with the observed purity of the construct. A further aspect that needs to be mentioned relates to the designed sequences and the conditions used to operate the logic gate. We have optimized the structure of the translocated mediator strands **2′** or **5′** or the ionic strength of the system to obtain maximal difference between the False, ′′0′′, and the True, ′′1′′, values (see optimization results in Supporting Information, Figures 1S, 2S). Finally, although the gate configuration consists of a complex structure composed of nine components, we find that the precise steps to setup the system and its activation at the defined conditions allow the result to be reproduced within a 15% error.

Figure 2A shows the activation of an "AND" gate, based on the DNA-translator platform. The construct of the "AND" system is very similar to that described for the "OR" system, except that the sequences constituting the mediator-strands **2′′** and **5′′**, and the footholds **3a** and **4a** that are hybridized with modified product-strands **3′′** and **4′′** are altered. Each of the product strands includes the half sequence of the HRP-mimicking DNAzyme. Thus, upon the activation of the system by either input **6** or **7**, and the subsequent release of DNAzyme halves **3′′** or **4′′**, respectively, the HRP-mimicking DNAzyme cannot be formed. Treatment of the system with both inputs releases, however, both fragments, **3′′** and **4′′**, and these self-assemble into the intermolecular G-quadruplex structure that yields, in the presence of hemin, the HRP-mimicking DNAzyme. That is, we make use of the fact that nucleic acid fragments may form complexes that yield catalytically active DNAzyme structures.[20] Figure 2B shows the time-dependent absorbance changes upon activation of the "AND" gate by the inputs **6**, **7**. Figure 2B, curves a, b, and c show the absorbance changes upon treatment of the system with no inputs, with input **6** only, and with input **7**, alone, correspondingly. Figure 2B, curve d, corresponds to the system activation with the two inputs. It is evident that upon treatment of the system with the two inputs (state 1, 1), the effective generation of the HRP-mimicking DNAzyme is achieved. Figure 2B, inset, shows the absorbance changes in the form of bars, and the derived truth table that corresponds to the "AND" gate.

We further extended the study by constructing the "XOR" gate using the DNA translator device activated by the two inputs **6** and **7**, as shown in Figure 3A. The DNA machine is very similar to the one used for the "OR" gate. Footholds **3** and **4** are hybridized here with two new designed product strands **3′′′** and **4′′′** that in-

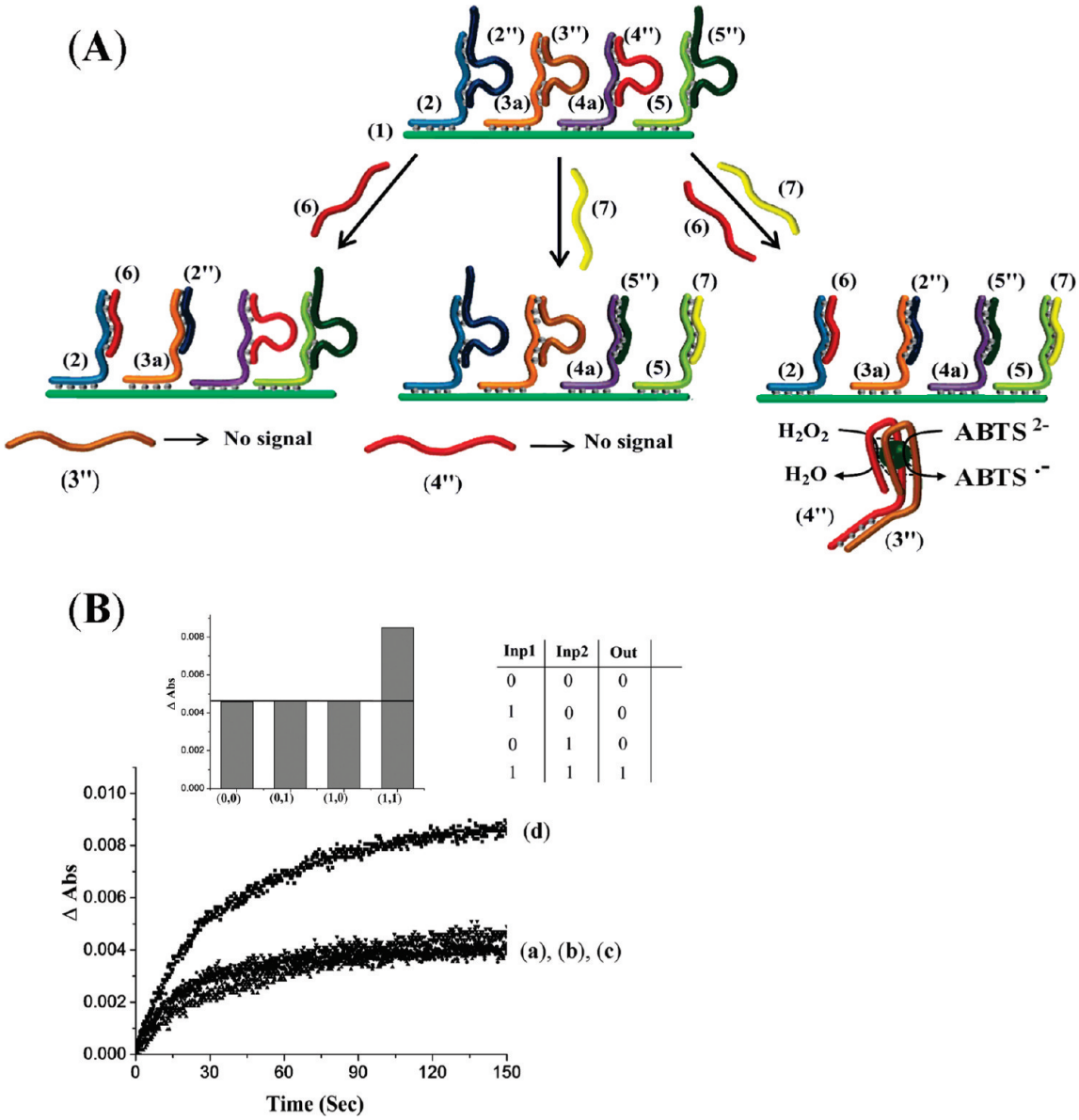

Figure 2. (A) Schematic presentation of an "AND" gate using a four-foothold nucleic acid structure on a DNA scaffold, and the activation of the logic gate by two-nucleic acids inputs. (B) Time-dependent absorbance changes stimulated by the released HRP-mimicking DNAzyme upon activation of the system by the respective nucleic acid inputs: (a) (0,0), (b) (0,1), (c) (1,0), (d) (1,1) (expressed as ΔAbs values, where ΔAbs corresponds to the difference between the absorbance generated by the input-activated system and the absorbance generated by hemin). Spectra recorded in the presence of hemin, 7×10^{-7} M, $ABTS^{2-}$, 2 mM, and H_2O_2, 2 mM. Results are presented in the inset in the form of a bar presentation and the respective truth-table.

clude, each, the HRP-mimicking DNAzyme sequence and additional complementary domains that can prevent the formation of the hemin-G quadruplex DNAzyme upon hybridization. The sequences **3**′′′ and **4**′′′ are blocked by partial hybridization with footholds **3** and **4**, and thus, the DNAzyme units are not activated. Thus, while either of the inputs **6** or **7** activates the formation of the HRP-mimicking DNAzyme, the introduction of both inputs leads to the displacement of two strands that mutually cancels the DNAzyme properties of each other through the formation of the duplex **3**′′′/**4**′′′.

Figure 3B shows the time-dependent absorbance changes of the system. The results confirm that the system performs the "XOR" gate function. Interaction of the system with either input **6** or **7** leads to the release of the HRP-mimicking DNAzymes, and to the catalyzed oxidation of $ABTS^{2-}$ to $ABTS^{\cdot-}$, curves b and c, respectively. Initiation of the system activity with both inputs **6** and **7** simultaneously, curve d, state (1, 1), leads to the low absorbance changes that are generated by the system also in the absence of any inputs, curve a. These results demonstrate that the system, indeed, performs the "XOR" gate operation (cf. absorbance bar presentation and the derived truth table, Figure 3B, inset).

In the second set of experiments, we substituted the nucleic acid inputs with the low-molecular-weight

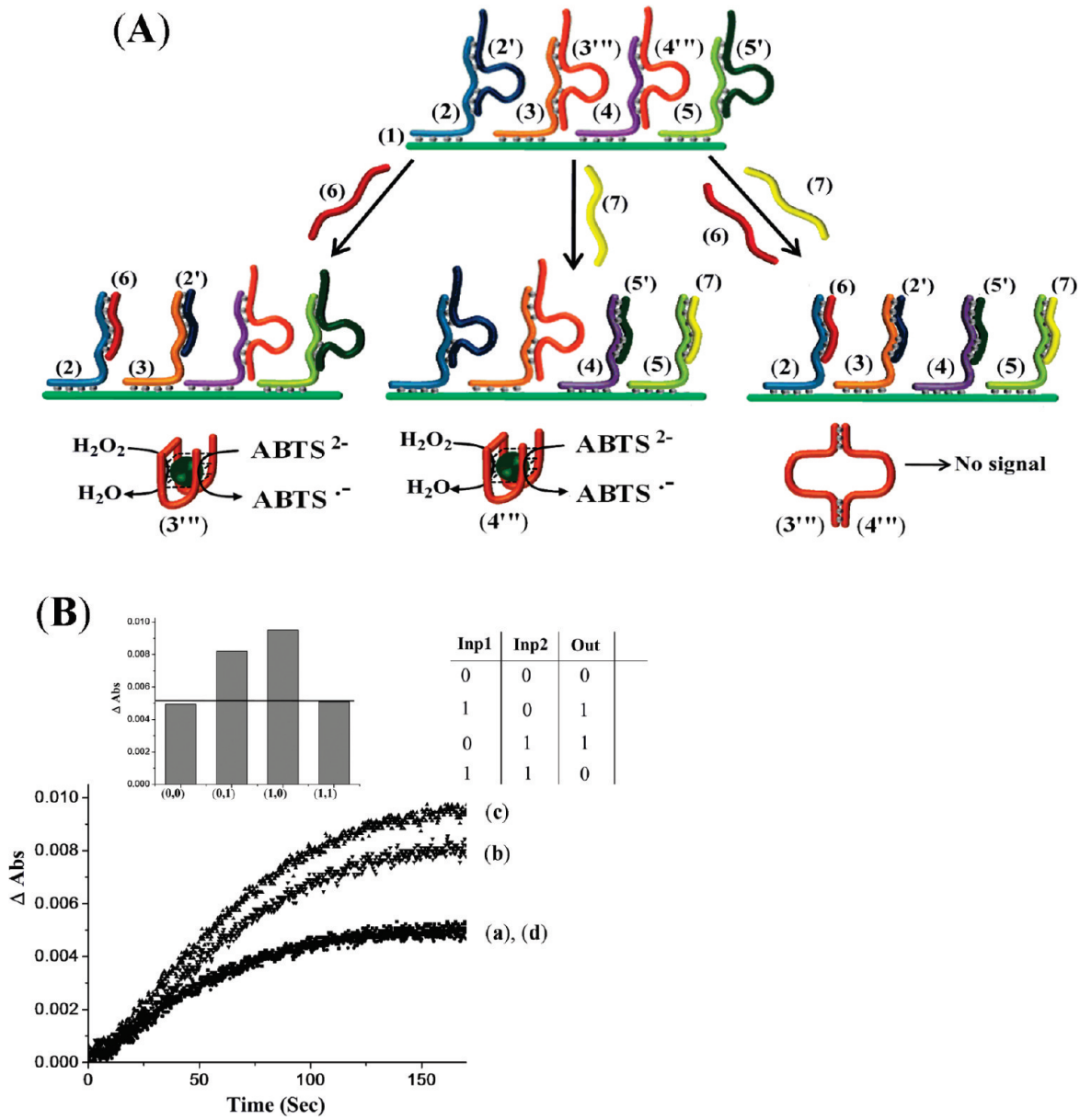

Figure 3. (A) Schematic presentation of an "XOR" gate using a four-foothold nucleic acid structure on a DNA scaffold, and the activation of the logic gate by two-nucleic acids inputs. (B) Time-dependent absorbance changes stimulated by the released HRP-mimicking DNAzyme upon activation of the system by the respective nucleic acid inputs: (a) (0,0), (b) (0,1), (c) (1,0), (d) (1,1) (expressed as ΔAbs values, where ΔAbs corresponds to the difference between the absorbance generated by the input-activated system and the absorbance generated by hemin). Spectra recorded in the presence of hemin, 7×10^{-7} M, $ABTS^{2-}$, 2 mM, and H_2O_2, 2 mM. Results are presented in the inset in the form of a bar presentation and the respective truth-table.

substrates, cocaine (CO) and adenosine monophosphate (AMP), and implemented the formation of input-aptamer complexes as initiators of the logic gate operations.

The "OR" gate machine, depicted in Figure 4A, is very similar to the one constructed for the DNA-inputs "OR" gate. The single-stranded tethers of footholds **2** and **5** were originally designed to include built-in aptamer sequences for cocaine (CO) or adenosine monophosphate (AMP), respectively. Footholds **3** and **4** are partially hybridized with the product-strands **3**′ and **4**′ that include, as a built-in component, the HRP-mimicking-DNAzyme sequence. The system is designed in such a way that prior to its activation by the inputs CO or AMP, mute state, (0,0), the duplexes **2**/**2**′ and **5**/**5**′ reveal enhanced stability as compared to the possible hybridization between **2**′/**3** or **5**′/**4**. The introduction of input molecules results in conformational changes of the corresponding aptamer foothold (**2** or **5**), formation of respective CO- or AMP-aptamer complex, and the displacement of corresponding mediator-strands (**2**′ or **5**′). The translocation of the mediator-strands **2**′ or **5**′ to footholds **3** or **4**, results in the displacement and the release of the product-strands **3**′ and **4**′, respectively, from the corresponding foothold. The displaced product-strands **3**′ or **4**′ self-assemble, in the presence

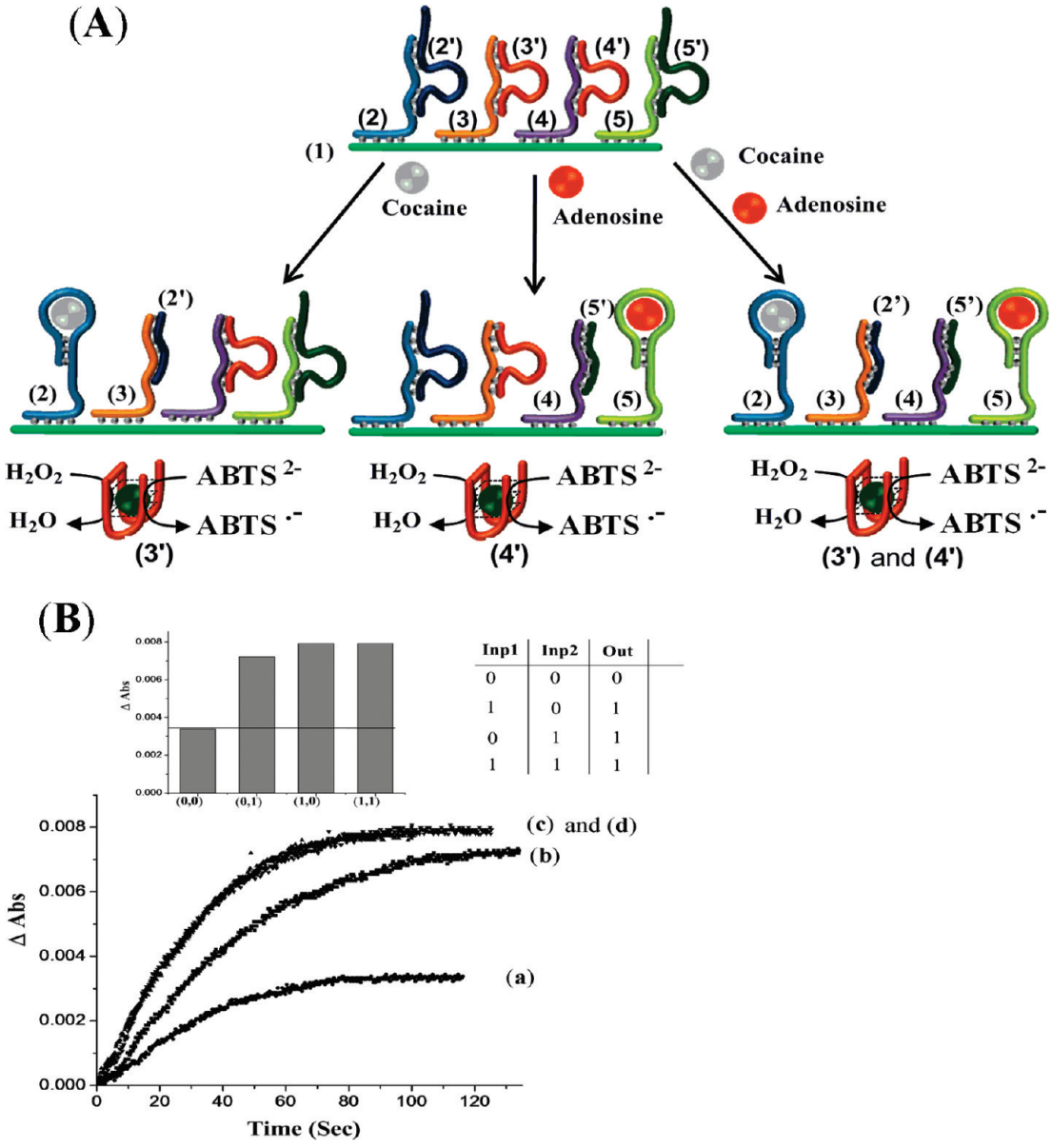

Figure 4. (A) Schematic presentation of an "OR" gate using a four-foothold nucleic acid structure on a DNA scaffold, and the activation of the logic gate by AMP and cocaine inputs. (B) Time-dependent absorbance changes stimulated by the released HRP-mimicking DNAzyme upon activation of the system by AMP and cocaine inputs (1.25×10^{-4}M): (a) (0,0), (b) (0,1), (c) (1,0), (d) (1,1). Spectra recorded in the presence of hemin, 7×10^{-7} M, $ABTS^{2-}$, 2 mM, and H_2O_2, 2 mM. Results are presented in the inset in the form of a bar presentation and the respective truth-table. ΔAbs corresponds to the difference between the absorbance generated by the input-activated system and the absorbance generated by hemin.

of hemin, to the hemin-G-quadruplex complex (HRP-mimicking-DNAzyme) that catalyzes the formation of the colored $ABTS^{\bullet-}$ product. Figure 4B shows the time-dependent evolution of $ABTS^{\bullet-}$ absorption upon activation of the system by the AMP or CO inputs, curves b and c, respectively, whereas curve d corresponds to the absorbance changes in the presence of the two inputs. The absorbance changes in the absence of the inputs, curve a, are due to residual DNAzyme units present in the solution. The absorbance changes in the form of bars and the truth table of the system are given in Figure 4B, inset.

One may realize that the system reveals the characteristics of an "OR" gate while the CO input displaces the DNAzyme **4**′ more effectively than the AMP input (see Figure 4B). The application of the two inputs, CO and AMP, results, however, in a similar absorbance to that of CO alone, although one would anticipate a higher readout signal than the response of any of the individual inputs, due to a higher content of the released DNAzyme. This is explained by the fact that the introduced CO and AMP molecules exhibit affinities to the released G-rich nucleic acids **3**′ and **4**′, and the formation of these complexes inhibits the formation of active DNAzymes (see details, Supporting Information, Figure 3S).

The assembly of the "AND" gate machine that is activated by the CO/AMP inputs is schematically depicted

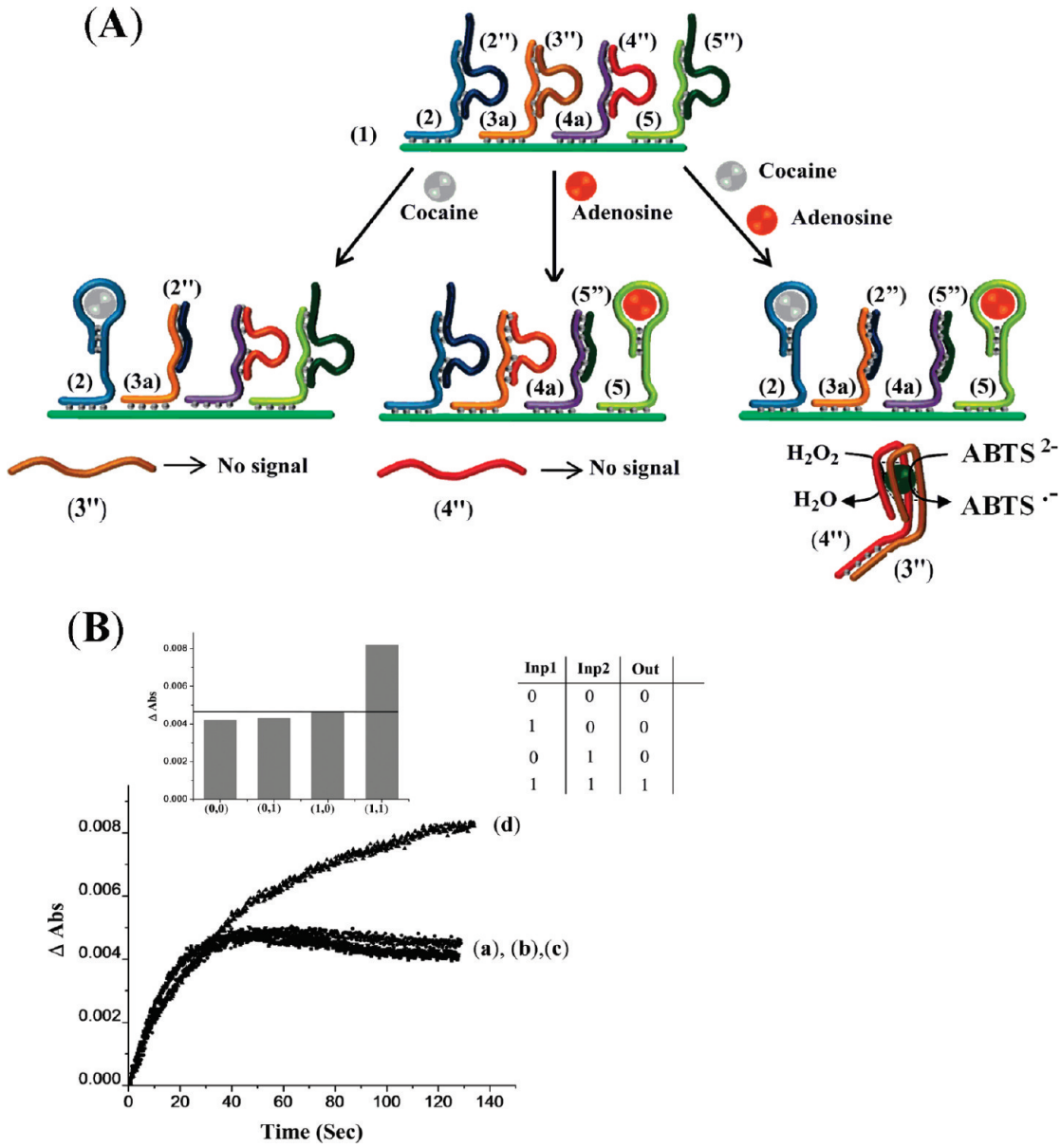

Figure 5. (A) Schematic presentation of an "AND" gate using a four-foothold nucleic acid structure on a DNA scaffold, and the activation of the logic gate by AMP and cocaine inputs. (B) Time-dependent absorbance changes stimulated by the released HRP-mimicking DNAzyme upon activation of the system by AMP and cocaine inputs (1.25×10^{-4}M): (a) (0,0), (b) (0,1), (c) (1,0), (d) (1,1). Spectra recorded in the presence of hemin, 7×10^{-7} M, $ABTS^{2-}$, 2 mM, and H_2O_2, 2 mM. Results are presented in the inset in the form of a bar presentation and the respective truth-table. ΔAbs corresponds to the difference between the absorbance generated by the input-activated system and the absorbance generated by hemin.

in Figure 5A. The system is very similar to that described for the "OR" gate, except that the base sequences in the mediator-strands **2**′′ and **5**′′ and the footholds **3a** and **4a** that are hybridized with modified product strands **3**′′ and **4**′′ are altered. Each of the product-strands consists of the half sequence of the HRP-mimicking DNAzyme. Thus, activating the system with only CO results in the formation of the respective CO-aptamer complex, and the translocation of the mediator-strand **2**′′ to foothold **3a**, while releasing product-strand **3**′′. The latter does not yield, however, any DNAzyme. Similarly, the treatment of the assembly with the AMP input yields the formation of the AMP-aptamer complex and the transfer of the mediator-strand **5**′′ to foothold **4a**, while releasing the product-strand **4**′′. As before, the released product-strand **4**′′ is catalytically inactive. The interaction of the DNA machine with the two inputs, CO and AMP, results, however, in the synchronized release of the product strands **3**′′ and **4**′′ that yields, in the presence of hemin, the intermolecular complex corresponding to the HRP-mimicking DNAzyme that catalyzes the formation of the colored $ABTS^{\bullet-}$ product. Figure 5B, curves a b, and c, show the time-dependent absorbance changes, as a result of formation of $ABTS^{\bullet-}$, upon treatment of the system with no inputs, with AMP only, and with CO

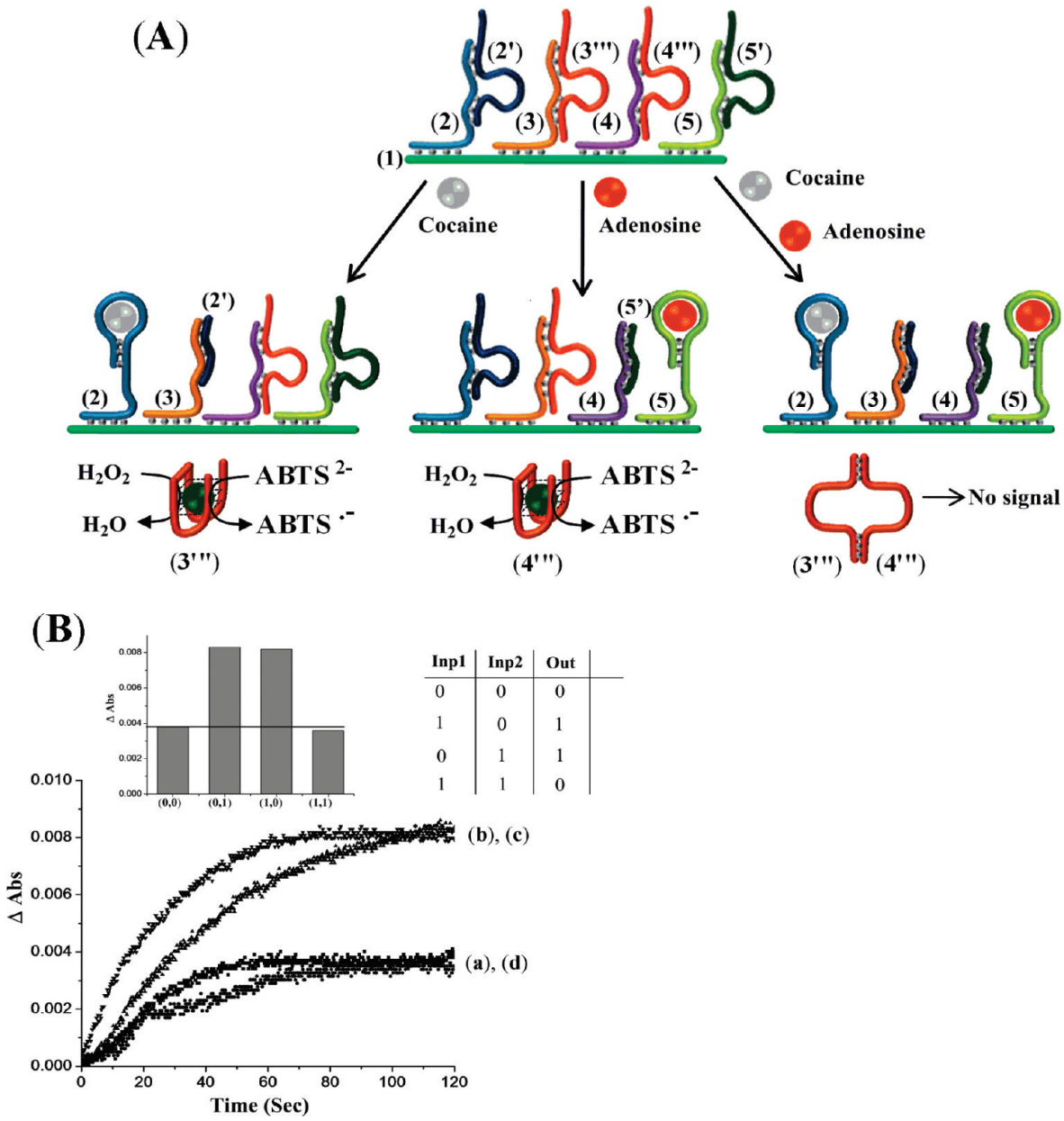

Figure 6. (A) Schematic presentation of an "XOR" gate using a four-foothold nucleic acid structure on a DNA scaffold and the activation of the logic gate by AMP and cocaine inputs. (B) Time-dependent absorbance changes stimulated by the released HRP-mimicking DNAzyme upon activation of the system by AMP and cocaine inputs (1.25×10^{-4}M): (a) (0,0), (b) (0,1), (c) (1,0), (d) (1,1). Spectra recorded in the presence of hemin, 7×10^{-7} M, $ABTS^{2-}$, 2 mM, and H_2O_2, 2 mM. Results are presented in the inset in the form of a bar presentation and the respective truth-table. ΔAbs corresponds to the difference between the absorbance generated by the input-activated system and the absorbance generated by hemin.

alone, respectively. Figure 5B, curve d, corresponds to the activation of the system with both inputs. It is evident that, upon treatment of the system with the two inputs, CO and AMP, (state 1,1) the HRP-mimicking DNAzyme is formed, resulting in the effective formation of $ABTS^{\bullet-}$, that represents a "True" output. Figure 5B, inset, shows the absorbance changes in the form of bars and the derived truth table of the "AND" gate.

The method to construct the challenging "XOR" gate is shown in Figure 6A. The assembly and the activation of the system is identical to the one described for the "XOR" gate with nucleic acids as inputs, albeit here the same footholds sequences, **2** and **5**, were implemented as aptamers for CO and AMP as inputs, respectively. The product-strands **3**′′′ and **4**′′′ include, each, the HRP-mimicking DNAzyme sequence and additional complementary domains. They are blocked by partial hybridization to footholds **3** and **4**, and thus, the DNAzyme units are catalytically inactive. Figure 6A shows the function of the system as the "XOR" gate. The interaction of the system with either CO or AMP yields the displacement of the product-strands, **3**′′′ or **4**′′′, leading to the active DNAzyme units, Figure 6B, curves b and c. Upon the introduction of both inputs,

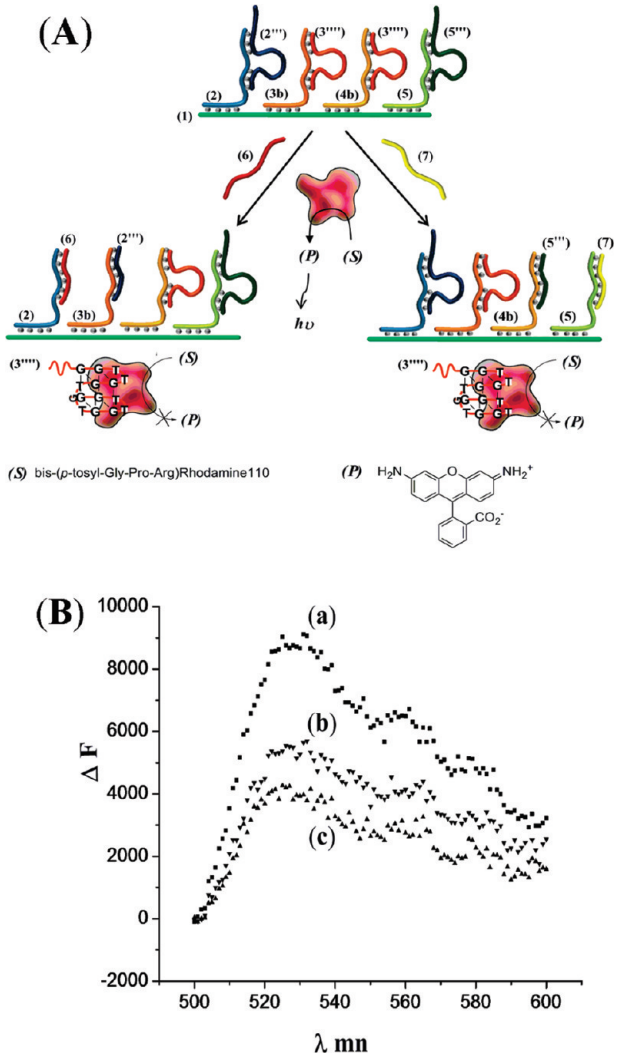

Figure 7. (A) The inhibition of thrombin by a DNA-based translator device where the antithrombin aptamer is released. (B) Fluorescence spectra corresponding to the thrombin-catalyzed hydrolysis of rhodamine110 bis(*p*-tosyl-Gly-Pro-Arg) in the presence of four-foothold nucleic acids associated with the DNA scaffold, in the absence of external nucleic acid activator (a), in the presence of nucleic acid 6 (b), or in the presence of nucleic acid 7 (c), as activators.

the release of the product-strand does not yield the active DNAzyme due to the intermolecular hybridization of **3**′′′ and **4**′′′, Figure 6B, curve d. The respective truth table and the absorbance changes in the form of bars are presented in Figure 6B, inset.

The previous systems addressed the construction of a set of DNA-scaffold-based logic gates that covers fundamental Boolean functions. It would be interesting, however, to suggest potential applications of such biomolecular systems. We propose that DNA-translator-based devices, that perform logic gate operations, might find future applications in nanomedicine. That is, the sensing of biomarkers for a certain disease should activate a translation process that releases predesigned nucleic acids that act either as antisense agents, or as inhibitors (aptamers) for harmful enzymes. For example, thrombin is a hydrolytic enzyme participating in blood clotting. It was reported that thrombin is generated in brain hemorrhage or trauma events, and that the generated thrombin could cause inflammatory brain diseases. Also, thrombin was found to play a role in edema formation and neurological deficits.[44] Thus, to introduce the scientific interlinks between nanomedicine and logics, we decided to use nucleic acid sequences as models for biomarkers that activate a DNA device, which releases the antithrombin aptamer that, in turn, inhibits the hydrolytic activity of thrombin.

In this machine, the track **1** and the footholds **2** and **5** are similar to those described in Figure 1A. The new footholds **3b** and **4b** are both hybridized with the same new product-strand **3**′′′′ that includes the antithrombin aptamer sequence (instead of the HRP-mimicking DNAzyme-containing sequences) (Figure 7A). Treatment of the functional track with the nucleic acids inputs **6** or **7** activates the translocation of the mediator-strands **2**′′′ or **5**′′′ to footholds **3b** or **4b** and the displacement, and release, of the antithrombin aptamer **3**′′′′, acting as product-strand. The formation of the aptamer−thrombin complexes inhibits, then, the hydrolytic activity of thrombin and prevents the thrombin-catalyzed hydrolysis of rhodamine110 bis(*p*-tosyl-Gly-Pro-Arg), Figure 7B. We realize that the DNA device, indeed, inhibits the hydrolytic activity of thrombin by *ca*. 40%, Figure 7B.

The performance of the DNA-scaffold-based device presents an example of integration of analytical and mechanical functions with model therapeutic effects. In principle, any aptamer substrate, or DNA sequence, can be used as the input of the device, and thus, biomarkers or a gene overexpression products in certain diseases could initiate the protein activity control.

CONCLUSIONS

Conjunction (“AND”), disjunction (“OR”), and exclusive disjunction (“XOR”) operations are the building blocks of Boolean logics; all other gates can be designed by suitable combinations of these logic functions. We have successfully constructed a set of DNA-based logic gates that encompasses these basic Boolean functions. The operations of these gates were readout by absorption spectroscopy. The modular design of the translators enables the adaptation of the DNA device to various input and output sequences. That is, nucleic acids, low-molecular-weight substrates, or macromolecules might act as inputs that activate the device through hybridization or by the formation of aptamer-substrate complexes. The major advance of the present study is the fact that the input and output entries do not interact one with another. Namely, the inputs translate into a mediator nucleic acid strand that affects the generation of the output strands. In previous studies, the input strand interacted directly with the displaced output strand on a common supporting strand[26] or did not generate any active output strand

but altered the fluorescence feature of a labeling fluorophore.[24,25] The benefits of uncoupled input and output strands are obvious, as the released strands might activate cascades of logic gates or could inhibit biocatalytic transformations. The suggestion to use the logic gate construct as a possible therapeutic tool for future nanomedicine is not free of obstacles. The degradation of the DNA structures by endonucleases is anticipated to introduce serious limitations (to the suggested method) by cleaving the released aptamers, DNAzymes, or nucleic acid inputs. The progress in protecting DNA structures against endonucleases by the introduction of non-natural bonds (*e.g.*, phosphorothioate linkages)[45] might be adapted in the future, to stabilize the DNA constructs on which the logic operations are activated. Also, while limited success was accomplished with antisense therapeutics, several studies advocated the use of DNAzymes or aptamers for intracellular applications.[46−48] The present approach might provide the seeds for the future evaluation of this paradigm.

The use of controlling elements that alter enzyme behavior is widespread in *in vivo* regulatory pathways. Future DNA-based control devices may include the use of DNA or aptamers acting as recognition elements for disease biomarkers and the development of antisense therapeutics against genes or protein-activated diseases. The suggested combination of both computational and controlling elements paves the way for the creation of more complex circuits, which could mimic natural systems through the use of diverse regulatory components.

MATERIALS AND METHODS

DNA Sequences.

(**1**) 5′-GGC AGA AAT TAC GGA AAG ACA GCG ACT CAA GCC ATT ATG GCA CGC CAT CAC GCG ATA TAG GCA GGC ATA AAC ACG CAG TTC TCA-3′
(**2**) 3′-CCC TCT GGG TGA AGT AAC TTC CTA AAT AGG AAC AGA GGG TCT TCT TCT CCG TAT TTG TGC GTC AAG AGT -5′
(**2**′) 5′-CAC TTT GGG AGA CCC ACG AAA TCT AAT TTG GCT CAT CCT AGA AGA AGA-3′
(**3**) 5′-TGC CTA TAT CGC GTG ATG GCG TTT TTT TTT T CCC AAC C GTGGG TCT CC C AAA GTG-3′
(**3**′ and **4**′) 5′-CA CTT TGG GTA GGG CGG GTT GGG-3′
(**4**) 5′-TGC CAT AAT GGC TTG AGT CGC TAA TAT T CCC AAC C C GAA GGTCC C AAA GTG-3′
(**5**′) 5′-CAC TTT G ACC TTC C GTG TTT TTT TTT TTT AGA AGA AGA-3′
(**5**) 5′ TGC CAT AAT GGC TTG AGT CGC TAA TTT TTAACCA ACC A GAG GAA GGTCC C AAA G TG-3′
(**6**) 5′-CC ACT TCA TTG AA T T AT TTA TCC TTG TCT CCC AGA AGA AG-3′
(**7**) 5′- CTC CGC AAT ACT CCC CCA GGT AGA AGA AG-3′
(**2**′′) 5′-GAAGA GGG AGA CCC ACG AAA TCT TTT TT GCT CTT CCT AGA AGA AGA-3′
(**3a**) 5′-TGC CTC TAT CGC GTG ATC GCG TTT TTT TTT T TA GTA GTA CGT GGG TCT CCC T CTT CCC-3′
(**4**) 5′-TGC CTA TAT CGC GTG ATG GCG TTT TTT TTT T CCC AAC C GTGGG TCT CC C AAA GTG-3′
(**3**′′) 5′-A GGG AC GGG AAG AAA GAT TTTTT GTAC TAC TA-3′
(**4a**) 5′-TGC CAT AAT GGC TTG AGT CGC TTT TTT TTT T T CCC AAT ACA CGA G GAA GG TA CTA CTA-3′
(**4**′′) 5′-TAG TAG TA TTTTT GCT CAA AAT TGG GAG GGT-3′
(**5**′′) 5′-TAG TA CC TTC CTC GTG TTC TTT TTT TTT TTT AGA AGA AGA-3′
(**4**′′′) 5′-CACTTT G CC GGG TA GGG C GGG TT GGG ATATAT-3′
(**3**′′′) 5′-TAT AT CAC TTT GGG TA GGG C GGG TT GGG C AAA G-3′
(**3b**) 5′- TGCCTATATCGCGTGATGGCGTTTTTTTTTTCCAACC AGT GGG TCT CCC AAAGTG-3′
(**2**′′′) 5′-CAC TTT GGG AGA CCC ACG ATA TCT AAT TTG CCT CAA TCT CAG AGA AG A AGA-3′
(**4b**) 5′- CCATAATGGCTTGAGTCGCTAATTTTTAACCAACCAGA-GGAAGGTC C A AAGTG-3′
(**4**′′′) 5′-CACTTTGGGACCTTCCTTGTGATCAATTTTTTTTTT-AGAAGAAGA-3′
(**3**′′′′) 5′- CTTTGGGGGTTGGTGTGGTTGG-3′

Materials. Oligonucleotides **1**−**3**′′′′ were custom-made and HPLC purified by Genosys (Sigma). Hemin was purchased from Porphyrin Products (Logan, UT) and used without further purification. A hemin stock solution was prepared in DMSO and stored in dark at −20 °C. Rhodamine110 bis(*p*-tosyl-Gly-Pro-Arg) was purchased from Molecular Probes (Eugene, Oregon). A stock solution of rhodamine110 bis(*p*-tosyl-Gly-Pro-Arg) was also prepared in DMSO and stored in dark at −20 °C. All chemicals, including thrombin from human plasma, tris(hydroxymethyl)aminomethane hydrochloride (Tris), 2,2′-azino-bis(3-ethylbenzothiazoline-6-sulfonic acid)-disodium salt, (ABTS), 4-(2-hydroxyethyl)piperazine-1 ethanesulfonic acid sodium salt (HEPES), and adenosine 5′-monophosphate (AMP) were purchased from Sigma and Aldrich, and used as supplied. Ultrapure water from NANOpure Diamond (Barnstead) source was used in all of the experiments.

Instrumental. Absorbance spectra were recorded using a Shimadzu UV-2401PC UV−vis spectrophotometer. Fluorescence spectra were taken on a photon counting spectrometer (Edinburgh Instruments, FLS 920), connected to a computer (F900 v. 6.3 software).

General Method. For the "OR" gate configuration, strands **1**, 2.4 $\times$ 10^{-6} M, **2** and **2**′, 1.4 $\times$ 10^{-6} M, were hybridized separately to yield the **2**/**2**′ foothold on the template **1** in Tris buffer 25 mM, pH = 8.2, 400 mM NaCl. The strands **3**/**3**′ and **4**/**4**′, 1.4 $\times$ 10^{-6} M, were hybridized in a separate compartment, and similarly the strands **5**/**5**′, 1.4 $\times$ 10^{-6} M, were hybridized in a separate compartment in Tris buffer 25 mM, pH = 8.2, 400 mM NaCl. All the different prehybridized samples were mixed together to yield the integrated four-foothold hybridized configuration shown in Scheme 2. The mixture was divided in four samples, and each was subjected to the respective oligonucleotide inputs **6** and **7**, 3.1 $\times$ 10^{-7} M: (0,0), (0,1), (1,0), (1,1), for a time interval of 30 min. From each of the samples 20 μL were transferred to a cuvette and diluted with Tris buffer 25 mM, pH = 8.2, 400 mM NaCl that included hemin, 7 $\times$ 10^{-7} M, $ABTS^{2-}$, 2 mM, and H_2O_2, 2 mM, to a final volume 220 μL. The time-dependent biocatalyzed oxidation of $ABTS^{2-}$ as a result of the activation respective inputs was recorded spectroscopically at λ = 414 nm.

For the "AND" gate configuration, oligonucleotides **1**,**2**′′ and **5**,**5**′′ were hybridized separately in Tris buffer 25 mM, pH = 8.2, 400 mM NaCl. Strands **3a**,**3**′′ and **4a**,**4**′′ were also hybridized in a separate compartment in Tris buffer 25 mM, pH = 8.2, 400 mM NaCl. All the different prehybridized samples were mixed together to yield the integrated four-foothold hybridized configuration shown in Figure 2A. The mixture was divided in four samples, and each was subjected to the respective nucleotide inputs **6** and **7**, (3.1 $\times$ 10^{-7} M): (0,0), (0,1), (1,0), (1,1), to time interval of 30 min. From each of the samples 20 μL were transferred to a cuvette and diluted with Hepes buffer 25 mM that included 50 mM KCl, 20 mM $MgCl_2$ to a final volume of 200 μL for time interval of 1 h for a G-quadraplex creation. Then hemin, 7 $\times$ 10^{-7} M, $ABTS^{2-}$, 2 mM, and H_2O_2, 2 mM, were added. The time-dependent biocatalyzed oxidation of $ABTS^{2-}$ as a result of the activation respective inputs was recorded spectroscopically at λ = 414 nm.

For the "XOR" gate configuration, strands **1**,**2**,**2**′ and **5**,**5**′ were hybridized separately to yield the **2**/**2**′ and **5**/**5**′ footholds on the template **1** in Tris buffer 25 mM, pH = 8.2, 400 mM NaCl. Strands **3**,**3**′′′ and **4**,**4**′′′ were also hybridized in a separate compartment in Tris buffer 25 mM, pH = 8.2, 400 mM NaCl. All the different prehybridized samples were mixed together to yield the integrated four-foothold hybridized configuration shown in Figure 3A. The mixture was divided in four samples, and each was subjected to the respective nucleotide inputs **6** and **7**, (3.1×10^{-7} M): (0,0), (0,1), (1,0), (1,1), to time interval of 30 min. From each of the samples 20 μL were transferred to a cuvette and diluted with Tris buffer 25 mM, pH = 8.2, 400 mM NaCl that included hemin, 7×10^{-7} M, $ABTS^{2-}$, 2 mM, and H_2O_2, 2 mM, to a final volume 220 μL. The absorbance measurements were recorded spectroscopically at λ = 414 nm.

In the second set of experiments the system was subjected to a low molecular weight substrates cocaine and AMP (1.25×10^{-4} M), that acted as a respective inputs: (0,0), (0,1), (1,0), (1,1), to time interval of 20 min. All logic gate configurations were built up by the same way, like it was described for the oligonucleotide inputs.

For the inhibition of thrombin by a DNA-based translator machine, oligonucleotides **1**,**2**,**2**′′′ and **5**,**5**′′′ were hybridized separately in Tris buffer 25 mM, pH = 7.4, 300 mM NaCl. Strands **3b**,**3**′′′′ and **4b**,**3**′′′′ were also hybridized in a separate compartment in Tris buffer 25 mM, pH = 7.4, 300 mM. All the different prehybridized samples were mixed together to yield the integrated four-foothold hybridized configuration shown in Figure 7A. From each of the samples 20 μL were transferred to a separate compartment and diluted with the thrombin binding buffer, included Tris-Ac 20 mM, 100 mM NaCl, 5 mM KCl, 1 mM $CaCl_2$, 1 mM $MgCl_2$, pH = 7.4 and thrombin 1×10^{-11} M was added to the system. For the fluorescence measurements chromogenic substrate rhodamine110 bis(*p*-tosyl-Gly-Pro-Arg) (S), 5.8×10^{-6} M, was used.

Acknowledgment. Parts of this research are supported by the EC MOLOC project and by the Naval Research Laboratory, USA.

Supporting Information Available: Improvement of the hybridization yields of the DNA construct by changing the ionic strength and by altering the degree of base-pairing in the system. Also, the effect of cocaine and adenosine monophosphate on the activity of the HRP-mimicking DNAzyme are provided. This material is available free of charge *via* the Internet at http://pubs.acs.org.

REFERENCES AND NOTES

1. Kuznetsov, A. M., Ulstrup, J. *Electron Transfer in Chemistry and Biology: an Introduction to the Theory*; John Wiley & Sons: New York, 1998.
2. Fromherz, P. Electrical Interfacing of Nerve Cells and Semiconductor Chips. *Chem. Phys. Chem.* **2002**, *3*, 276–284.
3. De Silva, A. P.; Uchiyama, S. Molecular Logic and Computing. *Nat. Nanotechnol.* **2007**, *2*, 399–410.
4. De Silva, A. P.; Vance, T. P.; West, M. E. S.; Wright, G. D. Bright Molecules with Sense, Logic, Numeracy and Utility. *Org. Biomol. Chem.* **2008**, *6*, 2468–2481.
5. Sauvage, J.-P. Transition Metal-Containing Rotaxanes and Catenanes in Motion: Toward Molecular Machines and Motors. *Acc. Chem. Res.* **1998**, *31*, 611–619.
6. Saha, S.; Stoddart, J. F. Photo-Driven Molecular Devices. *Chem. Soc. Rev.* **2007**, *36*, 77–92.
7. Shipway, A. N.; Willner, I. Electronically Transduced Molecular Mechanical and Information Functions on Surfaces. *Acc. Chem. Res.* **2001**, *34*, 421–432.
8. de Silva, A. P.; McClenaghan, N. D. Proof-of-Principle of Molecular-Scale Arithmetic. *J. Am. Chem. Soc.* **2000**, *122*, 3965–3966.
9. Remacle, F.; Levine, R. D. Quasiclassical Computation. *Proc. Natl. Acad. Sci. U.S.A.* **2004**, *101*, 12091–12095.
10. Credi, A.; Balzani, V.; Langford, S. J.; Stoddart, J. F. Logic Operations at the Molecular Level. An XOR Gate Based on a Molecular Machine. *J. Am. Chem. Soc.* **1997**, *119*, 2679–2681.
11. Joachim, C.; Gimzewski, J. K.; Aviram, A. Electronics Using Hybrid-Molecular and Mono-Molecular Devices. *Nature* **2000**, *408*, 541–548.
12. Baron, R.; Lioubashevski, O.; Katz, E.; Niazov, T.; Willner, I. Logic Gates and Elementary Computing by Enzymes. *J. Phys. Chem.* **2006**, *110*, 8451–8456.
13. Niazov, T.; Baron, R.; Katz, E.; Lioubashevski, O.; Willner, I. Concatenated Logic Gates Using Four Coupled Biocatalysts Operating in Series. *Proc. Natl. Acad. Sci. U.S.A.* **2006**, *46*, 17160–17163.
14. Baron, R.; Lioubashevski, O.; Katz, E.; Niazov, T.; Willner, I. Elementary Arithmetic Operations by Enzymes: A Model for Metabolic Pathway-Based Computing. *Angew. Chem., Int. Ed.* **2006**, *10*, 1572–1576.
15. Privman, V.; Strack, G.; Solenov, D.; Pita, M.; Katz, E. Biocomputing Security System: Concatenated Enzyme-Based Logic Gates Operating as a Biomolecular Keypad Lock. *J. Am. Chem. Soc.* **2008**, *130*, 4234–4235.
16. Ashkenazy, G.; Ghadiri, M. R. Boolean Logic Functions of a Synthetic Peptide Network. *J. Am. Chem. Soc.* **2004**, *126*, 11140–11141.
17. Wilson, D. S.; Szostak, J. W. *In Vitro* Selection of Functional Nucleic Acids. *Annu. Rev. Biochem.* **1999**, *68*, 611.
18. Famulok, M.; Mayer, G.; Blind, M. Nucleic Acid Aptamers - From Selection *in Vitro* to Applications *in Vivo*. *Acc. Chem. Res.* **2000**, *33*, 591.
19. Luzi, E.; Minunni, M.; Tombelli, S.; Mascini, M. New Trends in Affinity Sensing: Aptamers for Ligand Binding. *Trends Anal. Chem.* **2003**, *11*, 810–818.
20. Navani, N. K.; Li, Y. Nucleic Acid Aptamers and Enzymes as Sensors. *Curr. Opin. Chem. Biol.* **2006**, *10*, 272–281.
21. Emilsson, G. M.; Breaker, R. R. Deoxyribozymes: New Activities and New Applications. *Cell. Mol. Life Sci.* **2002**, *59*, 596–607.
22. Silverman, S. K. Catalytic DNA (Deoxyribozymes) for Synthetic Applications—Current Abilities and Future Prospects. *Chem. Commun.* **2008**, 3467–3485.
23. Willner, I.; Shlyahovsky, B.; Zayats, M.; Willner, B. DNAzymes for Sensing, Nanobiotechnology and Logic Gate Applications. *Chem. Soc. Rev.* **2008**, *37*, 1153–1165.
24. Stefanovic, D.; Stojanovic, M. N. A Deoxyribozyme-Based Molecular Automaton. *Nat. Biotechnol.* **2003**, *21*, 1069–1074.
25. Macdonald, J.; Li, Y.; Sutovic, M.; Lederman, H.; Pendri, K.; Lu, W.; Andrews, B. L.; Stefanovic, D.; Stojanovic, M. N. Medium Scale Integration of Molecular Logic Gates in an Autonomation. *Nano Lett.* **2006**, *6*, 2598–2603.
26. Voelcker, N. H.; Guckian, K. M.; Saghatelian, A.; Ghadiri, M. R. Sequence-Addressable DNA Logic. *Small* **2008**, *4*, 427–431.
27. Benenson, Y.; Paz-Elizur, T.; Adar, R.; Keinan, E.; Livneh, Z.; Shapiro, E. Programmable and Autonomous Computing Machine Made of Biomolecules. *Nature* **2001**, *414*, 430–434.
28. Adar, R.; Benenson, Y.; Linchiz, G.; Rosner, A.; Tishby, N.; Shapiro, E. Stochastic Computing with Biomolecular Automata. *Proc. Natl. Acad. Sci. U.S.A.* **2004**, *101*, 9960–9965.
29. Beissenhirtz, M.; Willner, I. DNA-Based Machines. *Org. Biomol. Chem.* **2006**, *4*, 3392–3401.
30. Bath, J.; Turberfield, A. J. DNA Nanomachines. *Nat. Nanotechnol.* **2007**, *2*, 275–284.
31. Seeman, N. C. From Genes to Machines: DNA Nanomechanical Devices. *Trends Biochem. Sci.* **2005**, *30*, 119–125.
32. Liedl, T.; Sobey, T. L.; Simmel, F. C. DNA-Based Nanodevices. *Nano Today* **2007**, *2*, 36–41.
33. Shin, J.-S.; Pierce, N. A. A Synthetic DNA Walker for Molecular Transport. *J. Am. Chem. Soc.* **2004**, *126*, 10834–10835.
34. Yurke, B.; Turberfield, A. J.; Mills, A. P.; Simmel, F. C.; Neumann, J. L. A DNA-Fuelled Molecular Machine Made of DNA. *Nature* **2000**, *406*, 605–608.

35. Tian, Y.; Mao, C. Molecular Gears: A Pair of DNA Circles Continuously Rolls Against Each Other. *J. Am. Chem. Soc.* **2004**, *126*, 11410–11411.
36. Elbaz, J.; Tel-Vered, R.; Freeman, R.; Yildiz, H. B.; Willner, I. Switchable Motion of DNA on Solid Supports. *Angew. Chem., Int. Ed.* **2009**, *1*, 133–137.
37. Beyer, S.; Simmel, F. C. A Modular DNA Signal Translator for the Controlled Release of a Protein by an Aptamer. *Nucleic Acids Res.* **2006**, *34*, 1581–1587.
38. Weizmann, Y.; Beissenhirtz, M. K.; Cheglakov, Z.; Nowarski, R.; Kotler, M.; Willner, I. A Virus Spotlighted by an Autonomous DNA Machine. *Angew. Chem., Int. Ed.* **2006**, *45*, 7384–7388.
39. Shlyahovsky, B.; Li, D.; Weizmann, Y.; Nowarski, R.; Kotler, M.; Willner, I. Spotlight of Cocaine by an Autonomous Aptamer-Based Machine. *J. Am. Chem. Soc.* **2007**, *129*, 3814–3815.
40. Li, D.; Wieckowska, A.; Willner, I. Optical Analysis of Hg^{2+} Ions by Oligonucleotide-Gold-Nanoparticle Hybrids and DNA-Based Machines. *Angew. Chem., Int. Ed.* **2008**, *47*, 3927–3931.
41. Seelig, G.; Soloveichik, D.; Zhang, D. Y.; Winfree, E. Enzyme-Free Nucleic Acid Logic Circuits. *Science* **2006**, *314*, 1585–1587.
42. Travascio, P.; Witting, P. K.; Mauk, A. G.; Sen, D. The Peroxidase Activity of Hemin-DNA Oligonucleotide Complex: Free Radical Damage to Specific Guanine Bases of the DNA. *J. Am. Chem. Soc.* **2001**, *123*, 1337–1348.
43. Travascio, P.; Li, Y. F.; Sen, D. A DNA-Enhanced Peroxidase Activity of a DNA Aptamer-Hemin Complex. *Chem. Biol.* **1998**, *5*, 505–517.
44. Chapman, J. Thrombin in Inflammatory Brain Diseases. *Autoimmunity Rev.* **2006**, *5*, 528–531.
45. Taylor, J. W.; Schmidt, W.; Cosstick, R.; Okruszeka, A.; Eckstein, F. The Use of Phosphorothioate-Modified DNA in Restriction Enzyme-Reactions to Prepare Nicked DNA. *Nucleic Acids Res.* **1985**, *13*, 8749–8764.
46. Win, N. W.; Smolk, C. D. Higher-Order Cellular Information Processing with Synthetic RNA Devices. *Science* **2008**, *322*, 456–460.
47. Chakraborti, S.; Banerjea, A. C. Inhibition of HIV-1 Gene Expression by Novel DNA Enzymes Targeted to Cleave HIV-1 TAR RNA: Potential Effectiveness Against all HIV-1 Isolates. *Mol. Ther.* **2003**, *7*, 817–826.
48. Dollins, C. M.; Nair, S.; Sullenger, B. A. Aptamers in Immunotherapy. *Hum. Gene Ther.* **2008**, *19*, 443–450.